

Optical properties of polaronic excitons in stacked quantum dots

V. N. Gladilin,* S. N. Klimin,* V. M. Fomin,*[†] and J. T. Devreese[‡]

Theoretische Fysica van de Vaste Stoffen, Departement Natuurkunde, Universiteit Antwerpen, Universiteitsplein 1, B-2610 Antwerpen, Belgium

(Received 4 August 2003; revised manuscript received 19 December 2003; published 27 April 2004)

We present a theoretical investigation of the optical properties of polaronic excitons in stacked self-assembled quantum dots, which is based on the nonadiabatic approach. A parallelepiped-shaped quantum dot is considered as a model for a self-assembled quantum dot in a stack. The exciton-phonon interaction is taken into account for all phonon modes specific for these quantum dots (bulklike, half space, and interface phonons). We show that the coupling between stacked quantum dots can lead to a strong enhancement of the optical absorption in the spectral ranges characteristic for phonon satellites.

DOI: 10.1103/PhysRevB.69.155325

PACS number(s): 78.67.Hc, 73.21.La

Nonadiabaticity is an inherent property of exciton-phonon systems in various quantum-dot structures. Nonadiabaticity drastically enhances the efficiency of the exciton-phonon interaction. The effects of nonadiabaticity are important to interpret the surprisingly high intensities of the phonon “sidebands” observed in the optical absorption, the photoluminescence, and the Raman spectra of quantum dots, in particular, an enhancement of these intensities with decreasing the quantum-dot size (see, e.g., Refs. 1 and 2). Deviations of intensities of the phonon-peak sidebands, observed in some experimental optical spectra, from the Franck-Condon progression, which is prescribed by the commonly used adiabatic approximation, find a natural explanation within our nonadiabatic approach.^{3–6} Recently, stacked quantum dots have received increasing attention (see, e.g., Refs. 7–13) due to the possibility to finely control their energy spectra. This makes stacked quantum dots very promising for future nanodevices.^{12,13} In the present work, the nonadiabatic approach is applied to stacked InAs/GaAs quantum dots, which reveal a richer structure of phonon and exciton spectra in comparison with those for a single quantum dot. Namely, in the stacked quantum dots, as distinct from a single quantum dot, the exciton (phonon) spectra contain groups of states (modes) of different symmetry with close energies (frequencies). Owing to small energy differences between the exciton energy levels within these groups, additional channels for nonadiabatic transitions as compared to a single quantum dot open in stacked quantum dots. Therefore, optical absorption spectra of stacked quantum dots contain more phonon satellites than those of a single quantum dot. These features of the optical absorption can be experimentally revealed, e.g., in the photoluminescence excitation measurements.

In order to model coupled self-assembled InAs/GaAs quantum dots, we consider a stack of N parallelepiped-shaped quantum dots with heights l_n ($n=2,4,\dots,2N$) and with the interdot distances l_n ($n=3,5,\dots,2N-1$) along the z axis. Within the present approach, the lateral sizes of each quantum dot in a stack are supposed to be much larger than its size l_n along the growth axis. The stack is a system of $(2N+1)$ layers ($n=1,\dots,2N+1$) with parameters

$$l_n, \varepsilon_n = \varepsilon_{\text{InAs}} \quad \text{for } n=2,4,\dots,2N,$$

$$l_n, \varepsilon_n = \varepsilon_{\text{GaAs}} \quad \text{for } n=3,5,\dots,2N-1,$$

$$l_n \rightarrow \infty, \varepsilon_n = \varepsilon_{\text{GaAs}} \quad \text{for } n=1,2N+1.$$

The bulklike optical-phonon frequencies in InAs and GaAs layers of the stacked InAs/GaAs quantum dots coincide with the LO-phonon frequencies in InAs and GaAs, respectively. The interface frequencies belong to the stacked quantum dots as a whole and satisfy the dispersion equation

$$\det \| a_{kn}(\omega) \| = 0 \quad (k,n=1,\dots,2N), \quad (1)$$

where $a_{kn}(\omega)$ is the dynamic matrix of the interface vibrations with the matrix elements

$$a_{nn}(\omega) = \varepsilon_n(\omega) \coth q_{\parallel} l_n + \varepsilon_{n+1}(\omega) \coth q_{\parallel} l_{n+1},$$

$$a_{n,n-1}(\omega) = a_{n-1,n}(\omega) = -\varepsilon_n(\omega) / \sinh q_{\parallel} l_n; \quad (2)$$

all other matrix elements are equal to zero.

In Fig. 1, typical interface-phonon spectra are represented for stacked InAs/GaAs quantum dots formed by two InAs parallelepipeds. The frequencies are plotted as a function of the in-plane wave number q_{\parallel} , which takes discrete values

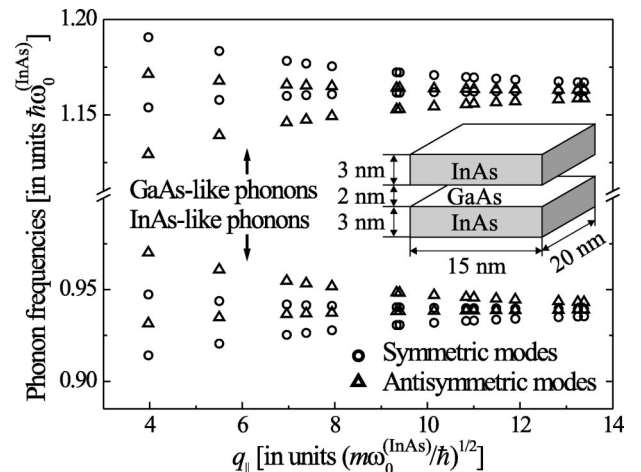


FIG. 1. Interface-phonon frequencies for two stacked parallelepiped-shaped InAs/GaAs quantum dots. $\omega_0^{(\text{InAs})}$ is the frequency of LO phonons in InAs at the center of the Brillouin zone.

due to the quantization of the phonons in the xy plane. In a stack of N quantum dots, each interface-phonon frequency of a single quantum dot splits into N branches. The splitting of the interface-phonon frequencies is due to the electrostatic interaction between the optical polar vibrations of the different quantum dots.

These features of the optical-phonon spectrum of stacked quantum dots are manifested in their optical properties. We calculate the optical absorption spectrum of polaronic excitons in stacked quantum dots starting from the Kubo formula. Within the nonadiabatic approach³ the following expression results for the linear coefficient of the optical absorption by the exciton-phonon system in a quantum-dot structure:

$$\alpha(\Omega) \propto \text{Re} \sum_{\beta, \beta'} d_{\beta}^* d_{\beta'} \int_0^{\infty} dt e^{i(\Omega - \Omega_{\beta} + i0^+)t} \langle \beta | \bar{U}(t) | \beta' \rangle, \quad (3)$$

where Ω is the frequency of the incident light, d_{β} and Ω_{β} are, respectively, the electric dipole matrix element and the Franck-Condon frequency of a transition between the exciton vacuum state and the one-exciton state $|\beta\rangle$. Exciton states in stacked InAs/GaAs quantum dots are determined using an exact diagonalization of the exciton Hamiltonian with simple parabolic valence and conduction bands within a finite-dimensional basis of the electron-hole states. The evolution operator averaged over the phonon ensemble $\bar{U}(t)$ is

$$\bar{U}(t) = T \exp \left\{ -\frac{1}{\hbar^2} \sum_{\lambda} \int_0^t dt_1 \int_0^{t_1} dt_2 \left[\frac{e^{-i\omega_{\lambda}(t_1-t_2)}}{1-y_{\lambda}} \gamma_{\lambda}(t_1) \right. \right. \\ \left. \left. \times \gamma_{\lambda}^{\dagger}(t_2) + \frac{y_{\lambda} e^{i\omega_{\lambda}(t_1-t_2)}}{1-y_{\lambda}} \gamma_{\lambda}^{\dagger}(t_1) \gamma_{\lambda}(t_2) \right] \right\}. \quad (4)$$

In Eq. (4), T is the time ordering operator, the index λ labels the phonon modes specific for the quantum-dot structure under consideration, ω_{λ} are phonon frequencies, $\gamma_{\lambda}(t)$ are the exciton-phonon interaction amplitudes in the interaction representation, and $y_{\lambda} = \exp(-\hbar\omega_{\lambda}/k_B T)$.

Within the adiabatic approximation, which has been widely used to calculate the optical spectra of quantum dots, nondiagonal matrix elements of the exciton-phonon interaction are neglected when calculating $\alpha(\Omega)$ as given by Eq. (3) with Eq. (4). In the adiabatic approach^{14,15} one supposes that (i) both the initial and the final states of a quantum transition are nondegenerate and (ii) the energy differences between the exciton states are much larger than the phonon energies. It has been shown in Refs. 3–6 that these conditions are often violated for optical transitions in small quantum dots, which have sizes less than the bulk exciton radius. In other words, the exciton-phonon system in a quantum dot can be essentially nonadiabatic. The polaron interaction for an exciton in a degenerate state results in internal nonadiabaticity (“the proper Jahn-Teller effect”), while the existence of exciton levels separated by an energy comparable with the LO-phonon energy leads to external nonadiabaticity (“the pseudo-Jahn-Teller effect”).

In general, the efficiency of the exciton-phonon interaction, as revealed through the optical spectra of quantum dots, depends on their geometric and material parameters in a complicated way. On the one hand, an increase of the confinement strength, which results from a decrease of the quantum-dot size or from a rise of potential barriers at the quantum-dot boundary, enhances the efficiency of the interaction with phonons for a solitary electron (a solitary hole). On the other hand, strengthening confinement leads to an increasing overlap between the electron and hole wave functions so that the net charge of the electron-hole pair and, correspondingly, the efficiency of the exciton-phonon interaction tend to decrease. As a result, the efficiency of the exciton-phonon interaction appears a nonmonotonous function of the confinement strength even within the adiabatic approximation (see, e.g., Ref. 16). Effects of nonadiabaticity, related to phonon-assisted transitions between different exciton states, drastically enhance intensities of phonon satellites in the optical spectra of quantum dots and, at the same time, make these intensities dependent on a vast set of parameters, which characterize the phonon-induced coupling between all the involved exciton states. Thus, side by side with the Fröhlich coupling constant α , energy spacing between exciton states strongly influences the aforementioned intensities. When the above spacing is comparable with the LO-phonon energy, nonadiabatic effects can strongly affect the optical spectra even in quantum dots of III-V semiconductor compounds, where the Fröhlich coupling constant is significantly smaller ($\alpha = 0.0504$ for InAs) than the values $\alpha \sim 0.5$ typical for II-VI semiconductors considered in Refs. 3 and 6.

In Ref. 3, a method was proposed to calculate the absorption spectrum given by Eqs. (3) and (4) taking into account the effect of nonadiabaticity on the probabilities of phonon-assisted optical transitions. The key step is the calculation of the matrix elements of the evolution operator $\langle \beta | \bar{U}(t) | \beta' \rangle$. In order to describe the effect of nonadiabaticity both on the intensities and on the positions of the absorption peaks, a diagrammatic approach can be used. When calculating these matrix elements we take into account that in a quantum dot, due to the absence of momentum conservation, the product $\langle \beta_1 | \gamma_{\lambda} | \beta_2 \rangle \langle \beta_2 | \gamma_{\lambda}^* | \beta_3 \rangle$ can be nonzero for $\beta_1 \neq \beta_3$, as distinct from the bulk case. Consequently, the evolution operator is, in general, nondiagonal in the basis of one-exciton wave functions $|\beta\rangle$. For the absorption coefficient we obtain

$$\alpha(\Omega) \propto -\text{Im} \sum_{\beta} |d_{\beta}|^2 G_{\beta}(\Omega + i0^+) - \text{Im} \sum_{\beta, \beta'} d_{\beta} d_{\beta'}^* \\ \times [\mathcal{Q}_{\beta\beta'}^{(1)}(\Omega + i0^+) + \mathcal{Q}_{\beta\beta'}^{(2)}(\Omega + i0^+)], \quad (5)$$

where

$$G_{\beta}(\Omega) = \sum_{\{j_{\lambda} = -\infty\}}^{\{\infty\}} C_{\{j_{\lambda}\}\beta}^{(+)} \left[\Omega - \Omega_{\beta} + \sum_{\lambda} S_{\lambda, \beta} \omega_{\lambda} - \sum_{\lambda} j_{\lambda} \omega_{\lambda} \right. \\ \left. - \sum_{\beta}^{(1)} \left(\Omega - \sum_{\lambda} j_{\lambda} \omega_{\lambda} \right) - \sum_{\beta}^{(2)} \left(\Omega - \sum_{\lambda} j_{\lambda} \omega_{\lambda} \right) \right]^{-1}, \quad (6)$$

$$C_{\{j_\lambda\}\beta}^{(\pm)} = \prod_{\lambda} (\pm 1)^{j_\lambda} \exp \left[\mp (2\bar{n}_\lambda + 1) S_{\lambda\beta} + \frac{j_\lambda \hbar \omega_\lambda}{2k_B T} \right] \times I_{|j_\lambda|} \left(S_{\lambda\beta} \left[2 \sinh \left(\frac{\hbar \omega_\lambda}{2k_B T} \right) \right]^{-1} \right). \quad (7)$$

$I_n(x)$ is a modified Bessel function of the first kind and $S_{\lambda\beta}$ is the Huang-Rhys parameter, which is related to the interaction of the exciton in the state β with phonons of the λ th mode:

$$S_{\lambda\beta} = \left| \frac{\langle \beta | \gamma_\lambda | \beta \rangle}{\hbar \omega_\lambda} \right|^2. \quad (8)$$

The self-energy terms $\Sigma_\beta^{(1)}(\Omega)$ and $\Sigma_\beta^{(2)}(\Omega)$ in Eq. (6) are obtained by summing diagrams, which describe one- and two-phonon nonadiabatic contributions,

$$\Sigma_\beta^{(1)}(\Omega) = \sum_{j=\pm 1} \sum_{\lambda, \beta_1} F_{\beta\beta_1}(\Omega - j\omega_\lambda) M_{\lambda\beta\beta_1\beta_1\beta}^{(j)} \quad (9)$$

and

$$\begin{aligned} \Sigma_\beta^{(2)}(\Omega) &= \sum_{j_1, j_2=\pm 1} \sum_{\lambda_1, \lambda_2} \sum_{\beta_1, \beta_2, \beta_3} F_{\beta\beta_1}(\Omega - j_1\omega_{\lambda_1}) \\ &\times F_{\beta\beta_3}(\Omega - j_2\omega_{\lambda_2}) [F_{\beta\beta_2}(\Omega - j_1\omega_{\lambda_1} - j_2\omega_{\lambda_2}) \\ &\times M_{\lambda_1\beta\beta_1\beta_2\beta_3}^{(j_1)} M_{\lambda_2\beta_1\beta_2\beta_3\beta}^{(j_2)} + F_{\beta\beta_2}(\Omega) \\ &\times M_{\lambda_1\beta\beta_1\beta_1\beta_2}^{(j_1)} M_{\lambda_2\beta_2\beta_3\beta_3\beta}^{(j_2)} (1 - \delta_{\beta_2\beta})], \end{aligned} \quad (10)$$

where

$$F_{\beta\beta_1}(\Omega) = \sum_{\{j_\lambda=-\infty\}}^{\{\infty\}} C_{\{j_\lambda\}\beta}^{(-)} G_{\beta_1} \left(\Omega - \sum_{\lambda} j_\lambda \omega_\lambda \right), \quad (11)$$

$$M_{\lambda\beta_1\beta_2\beta_3\beta_4}^{(j)} = m_{\lambda\beta_1\beta_2\beta_3\beta_4}^{(j)} - m_{\lambda\beta_1\beta_1\beta_1\beta_1}^{(j)} \delta_{\beta_1\beta_2} \delta_{\beta_3\beta_4}, \quad (12)$$

$$m_{\lambda\beta_1\beta_2\beta_3\beta_4}^{(j)} = \frac{j \langle \beta_{2-j} | \gamma_\lambda | \beta_{3-j} \rangle \langle \beta_{2+j} | \gamma_\lambda^\dagger | \beta_{3+j} \rangle}{\hbar^2 (1 - y_\lambda^j)}. \quad (13)$$

The above restriction to one- and two-phonon contributions is justified when the nonadiabatic exciton-phonon interaction is weak: $|\langle \beta | \gamma_\lambda | \beta' \rangle|^2 \ll \hbar \omega_\lambda$ for $\beta' \neq \beta$. The functions $Q_{\beta\beta'}^{(1)}(\Omega)$ and $Q_{\beta\beta'}^{(2)}(\Omega)$ in Eq. (5), which describe contributions of one- and two-phonon processes to nondiagonal matrix elements of the evolution operator, take the form

$$\begin{aligned} Q_{\beta\beta'}^{(1)}(\Omega) &= G_\beta(\Omega) G_{\beta'}(\Omega) (1 - \delta_{\beta\beta'}) \\ &\times \sum_{j=\pm 1} \sum_{\lambda, \beta_1} G_{\beta_1}(\Omega - j\omega_\lambda) m_{\lambda\beta\beta_1\beta_1\beta'}^{(j)}, \end{aligned} \quad (14)$$

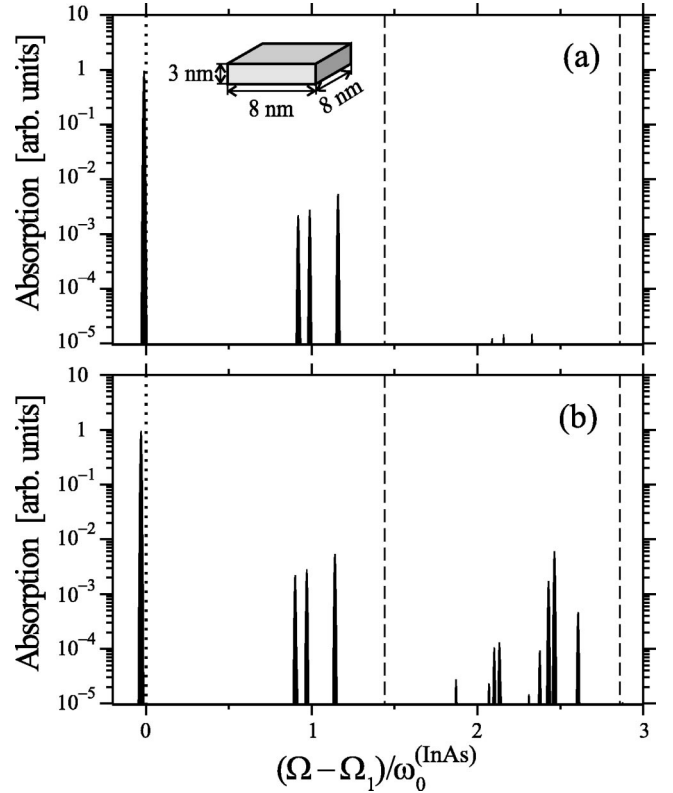


FIG. 2. Absorption spectra, calculated with the adiabatic approximation [panel (a)] and with the nonadiabatic approach [panel (b)] for a single quantum dot. Optically active and nonactive energy levels of a bare exciton are shown as dotted and dashed lines, respectively. Ω_1 is the transition frequency for the lowest state of a bare exciton.

$$\begin{aligned} Q_{\beta\beta'}^{(2)}(\Omega) &= G_\beta(\Omega) G_{\beta'}(\Omega) (1 - \delta_{\beta\beta'}) \\ &\times \sum_{j_1, j_2=\pm 1} \sum_{\lambda_1, \lambda_2} \sum_{\beta_1, \beta_2, \beta_3} G_{\beta_1}(\Omega - j_1\omega_{\lambda_1}) \\ &\times G_{\beta_3}(\Omega - j_2\omega_{\lambda_2}) \{ G_{\beta_2}(\Omega - j_1\omega_{\lambda_1} - j_2\omega_{\lambda_2}) \\ &\times [(1 - \delta_{\beta_3\beta_1}) m_{\lambda_1\beta\beta_1\beta_3\beta'}^{(j_1)} m_{\lambda_2\beta_1\beta_2\beta_3\beta}^{(j_2)} \\ &+ m_{\lambda_1\beta\beta_1\beta_2\beta_3}^{(j_1)} m_{\lambda_2\beta_1\beta_2\beta_3\beta'}^{(j_2)}] + G_{\beta_2}(\Omega) (1 - \delta_{\beta_2\beta}) \\ &\times (1 - \delta_{\beta_2\beta'}) m_{\lambda_1\beta\beta_1\beta_1\beta_2}^{(j_1)} m_{\lambda_2\beta_2\beta_3\beta_3\beta'}^{(j_2)} \}. \end{aligned} \quad (15)$$

The absorption spectrum is thus expressed through the functions $G_\beta(\Omega)$, which in turn are determined by a closed set of equations, Eq. (6) and Eqs. (9)–(11).

In Figs. 2, 3, and 4 the calculated optical absorption spectra are shown for a single quantum dot, two stacked identical quantum dots, and two stacked dots with somewhat different heights, respectively. The calculations were performed for low temperatures, $\{y_\lambda \ll 1\}$, when the absorption-line broadening due to the exciton-LO-phonon interaction is negligible. The broadening shown in Figs. 2–4 is introduced only to enhance visualization. From the comparison of the spectra obtained in the adiabatic approximation with those resulting

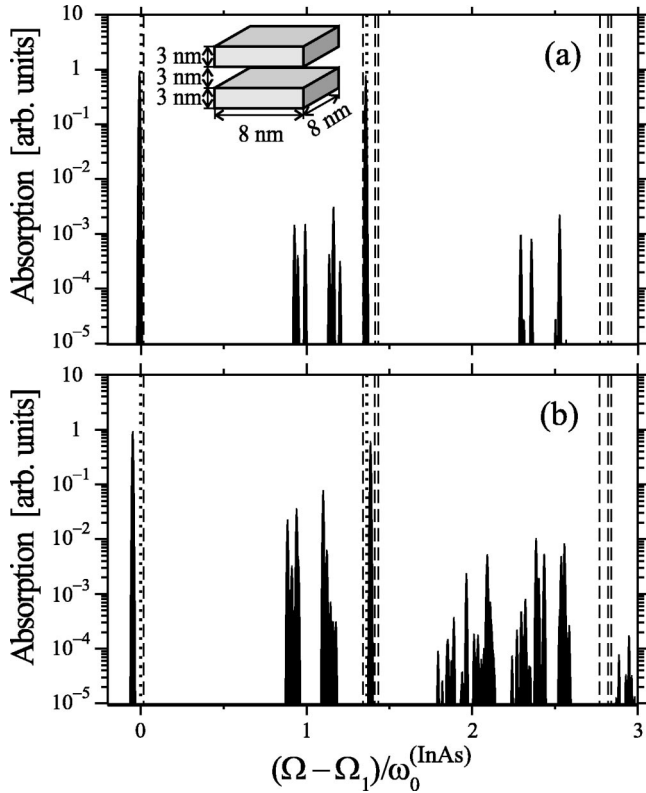


FIG. 3. Absorption spectra, calculated with the adiabatic approximation [panel (a)] and with the nonadiabatic approach [panel (b)] for two stacked identical quantum dots. Notations are the same as in Fig. 2.

from the nonadiabatic approach, the following effects of nonadiabaticity are revealed. First, the polaron shift of the zero-phonon lines with respect to the bare-exciton levels is larger in the nonadiabatic approach than in the adiabatic approximation. Second, there is a strong increase of the intensities of the phonon satellites compared to those given by the adiabatic approximation. This increase can be by more than two orders of magnitude. Third, in the optical absorption spectra found within the nonadiabatic approach, there appear phonon satellites related to nonactive bare exciton states.

Fourth, the optical-absorption spectra demonstrate the crucial role of nonadiabatic mixing of different exciton and phonon states in quantum dots. This results in a rich structure of the absorption spectrum of the exciton-phonon system.^{4,5,17} For the stacked quantum dots, this effect is significantly enhanced when the exciton-level splitting, caused by the coupling between quantum dots, is comparable with a LO-phonon energy [see Figs. 3(b) and 4(b)]. Similar conclusions about the influence of the exciton-phonon interaction on the optical spectra of quantum dots have been recently formulated in Ref. 18 for the “strong coupling regime” for excitons and LO phonons. Such a strong coupling regime is a particular case of the nonadiabatic mixing related to a resonance, which arises when the spacing between exciton levels is close to the LO-phonon energy. As seen from Figs. 3 and 4, effects of nonadiabaticity lead to a significant increase of absorption peaks in the spectral ranges, characteristic for one- and two-phonon satellites, even in the case when the

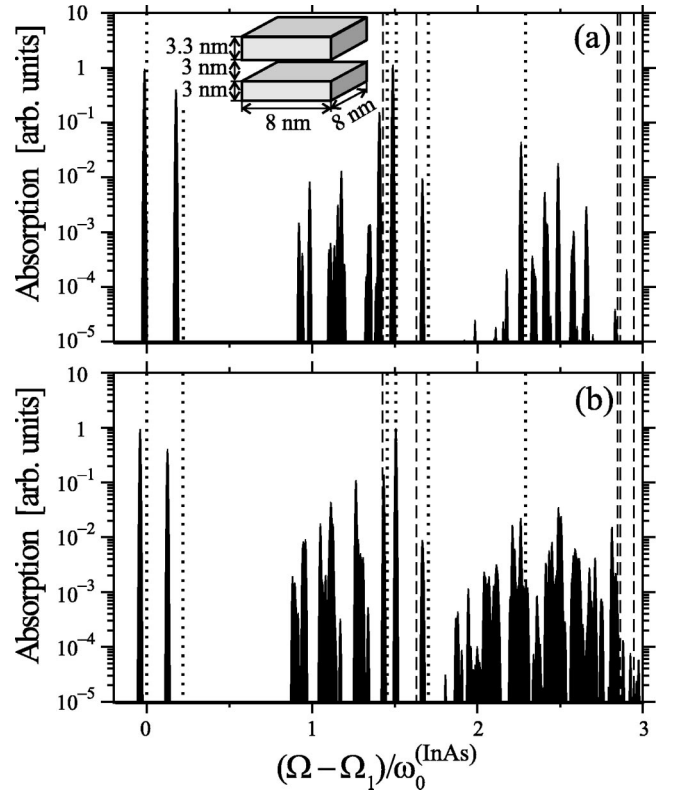


FIG. 4. Absorption spectra, calculated with the adiabatic approximation [panel (a)] and with the nonadiabatic approach [panel (b)] for two stacked quantum dots of different height. Notations are the same as in Fig. 2.

exciton-level spacing is relatively far from satisfying the aforementioned resonant conditions.

In some cases (see, e.g., Ref. 3) the luminescence spectrum of a quantum dot can be easily derived from its absorption spectrum. For example, under the assumption that the distribution function of the states of an exciton coupled to the phonon field, $f(\Omega)$, depends only on the energy of a state, the luminescence intensity at low temperatures ($\{y_\lambda \ll 1\}$) can be represented as

$$I(\Omega) \propto \sum_{K=0}^{\infty} \frac{1}{K!} \sum_{\lambda_1, \dots, \lambda_K} f\left(\Omega + \sum_{k=0}^K \omega_{\lambda_k}\right) \times \left(\prod_{k=1}^K \frac{\partial}{\partial y_{\lambda_k}} \right) \alpha(\Omega) \Big|_{\{y_\lambda \rightarrow 0\}}. \quad (16)$$

Equation (16) is applicable, for instance, for thermodynamic equilibrium photoluminescence. In this case the radiative lifetime of an exciton is much larger than the time characteristic of radiationless relaxation between one-exciton states.

We have calculated the spectra of thermodynamic equilibrium luminescence at $T \rightarrow 0$ (not shown here) for quantum dots with parameters indicated above. Both for single and for coupled quantum dots, the intensities of phonon satellites in these spectra are significantly smaller than in the absorption spectrum. This is because in quantum dots under consideration the lowest one-exciton energy level (with $\beta=1$) is less

affected by the phonon-induced nonadiabatic mixing of states than higher levels. The luminescence spectrum at zero temperature is determined by transitions from the state with $\beta=1$, while the absorption spectrum contains appreciable contributions due to transitions to higher exciton-phonon states.

Due to nonadiabaticity, multiple absorption peaks appear in the spectral ranges characteristic for phonon satellites. From the states, which correspond to these peaks, the system can rapidly relax to the lowest emitting state. Therefore, in the photoluminescence excitation (PLE) spectra of quantum dots, pronounced peaks can be expected in spectral ranges characteristic for phonon satellites. Experimental evidence of

the enhanced phonon-assisted absorption due to nonadiabaticity has been recently provided by PLE measurements on single self-assembled InAs/GaAs (Ref. 19) and InGaAs/GaAs (Ref. 20) quantum dots. Our results, which imply significantly more pronounced phonon satellites in PLE spectra compared to the luminescence spectra from the lowest one-exciton state, are in line with the experimental observations.^{19,20}

This work was supported by the GOA BOF UA 2000, I.U.A.P., F.W.O.-V. Projects G.0274.01N, G.0435.03, the W.O.G. Project No. WO.025.99N (Belgium), and the European Commission GROWTH Program, NANOMAT Project, Contract No. G5RD-CT-2001-00545.

*Permanent address: Department of Theoretical Physics, State University of Moldova, Str. A. Mateevici 60, MD-2009 Kishinev, Republic of Moldova.

†Also at Technische Universiteit Eindhoven, P. B. 513, 5600 MB Eindhoven, The Netherlands.

¹V. Jungnickel and F. Henneberger, *J. Lumin.* **70**, 238 (1996).

²M. Bissiri, G. Baldassarri Höger von Högersthal, A.S. Bhatti, M. Capizzi, A. Frova, P. Frigeri, and S. Franchi, *Phys. Rev. B* **62**, 4642 (2000).

³V.M. Fomin, V.N. Gladilin, J.T. Devreese, E.P. Pokatilov, S.N. Balaban, and S.N. Klimin, *Phys. Rev. B* **57**, 2415 (1998).

⁴J.T. Devreese, V.M. Fomin, V.N. Gladilin, E.P. Pokatilov, and S.N. Klimin, *Nanotechnology* **13**, 163 (2002).

⁵J.T. Devreese, V.M. Fomin, E.P. Pokatilov, V.N. Gladilin, and S.N. Klimin, *Phys. Status Solidi C* **0**, 1189 (2003).

⁶E.P. Pokatilov, S.N. Klimin, V.M. Fomin, J.T. Devreese, and F.W. Wise, *Phys. Rev. B* **65**, 075316 (2002).

⁷T. Schmidt, R.J. Haug, K. von Klitzing, A. Förster, and H. Lüth, *Phys. Rev. Lett.* **78**, 1544 (1997).

⁸R.J. Luyken, A. Lorke, M. Fricke, J.P. Kotthaus, G. Medeiros-Ribeiro, and P.M. Petroff, *Nanotechnology* **10**, 14 (1999).

⁹B. Partoens and F.M. Peeters, *Phys. Rev. Lett.* **84**, 4433 (2000).

¹⁰M. Pi, A. Emperador, M. Barranco, F. Garcias, K. Muraki, S.

Tarucha, and D.G. Austing, *Phys. Rev. Lett.* **87**, 066801 (2001).

¹¹M. Bayer, P. Hawrylak, K. Hinzer, S. Fafard, M. Korkusinski, Z.P. Wasilewski, O. Stern, and A. Forchel, *Science* **297**, 1313 (2002).

¹²L. Rebohle, F.F. Schrey, S. Hofer, G. Strasser, and K. Unterrainer, *Appl. Phys. Lett.* **81**, 2079 (2002).

¹³S. Bednarek, T. Chwiej, J. Adamowski, and B. Szafran, *Phys. Rev. B* **67**, 205316 (2003).

¹⁴S.I. Pekar, *Zh. Eksp. Teor. Fiz.* **20**, 267 (1950).

¹⁵K. Huang and A. Rhys, *Proc. R. Soc. London, Ser. A* **204**, 406 (1950).

¹⁶S. Nomura and T. Kobayashi, *Phys. Rev. B* **45**, 1305 (1992).

¹⁷V.N. Gladilin, S.N. Balaban, V.M. Fomin, and J.T. Devreese, in *Proceedings of the 25th International Conference on the Physics of Semiconductors, Osaka, Japan, 2000*, edited by N. Miura and T. Ando (Springer, Berlin, 2001), Part II, pp. 1243 and 1244.

¹⁸O. Verzelen, R. Ferreira, and G. Bastard, *Phys. Rev. Lett.* **88**, 146803 (2002).

¹⁹A. Lemaître, A.D. Ashmore, J.J. Finley, D.J. Mowbray, M.S. Skolnick, M. Hopkinson, and T.F. Krauss, *Phys. Rev. B* **63**, 161309 (2001).

²⁰A. Zrenner, F. Findeis, M. Baier, M. Bichler, and G. Abstreiter, *Physica B* **298**, 239 (2001).